

IR-UWB 패킷 기반의 Ranging 시스템을 위한 주파수 오프셋 추정기

정희원 오미경*, 김재영*, 이형수*

Frequency Offset Estimation for IR-UWB Packet-Based Ranging System

Mi-Kyung Oh*, Jae-Young Kim*, HyungSoo Lee* *Regular Members*

요약

본 논문에서는 IEEE 802.15.4a IR-UWB Ranging 시스템을 위한 주파수 오프셋 추정기를 제안한다. 주파수 오프셋 추정은 실내 다중경로 환경에서의 고정밀 Ranging을 위해 반드시 필요한 것으로 IEEE 802.15.4a 시스템에 적합한 주파수 오프셋 추정기의 제안이 필수이다. 먼저 IR-UWB 패킷에서 Ternary 프리앰블 코드 특징을 이용하여 ML 기반 주파수 오프셋 추정기를 제안하고, 하드웨어 구현을 위해 복잡도가 낮은 주파수 오프셋 추정기를 제안한다. 제안된 두 개의 주파수 오프셋 추정기 성능을 확인하기 위하여 이론적 분석을 수행하였고, IEEE 802.15.4a 다중 경로 채널 모델을 이용한 시뮬레이션을 통하여 다중 경로 환경에서도 주파수 오프셋 추정 성능이 우수함을 증명한다.

Key Words : IR-UWB, Ranging, Frequency Offset Estimation

ABSTRACT

We aim at frequency offset estimation for IEEE 802.15.4a ranging systems, where an impulse-radio ultra-wideband (IR-UWB) signal is exploited, By incorporating the property of the ternary code in the preamble, we derive a simplified maximum-likelihood (ML) estimation of the frequency offset. In addition, a closed form estimator for implementation is investigated. Simulation results and theoretical analysis verify our estimators in IEEE 802.15.4a IR-UWB packet-based ranging systems.

I. Introduction

Recently, impulse-radio ultra-wideband(IR-UWB) has been selected as a physical layer by IEEE 802.15.4a for the purpose of low-rate communication and ranging^[1]. The benefits of IR-UWB include the following: a) the possibility of low-cost low-power transceiver, b) better immunity from multipath propagation, c) accurate ranging, and d)

low interference^{[2],[3]}.

However, there are still many technical challenges that need to be solved for widespread deployment of an IR-UWB system^[2]. Estimating and compensating a frequency offset, which is called frequency synchronization, is one of the tasks that must be performed at an IR-UWB coherent receiver. Although IEEE 802.15.4a supports modulation schemes for both coherent

* 본 연구는 지식경제부 및 한국산업기술평가관리원의 IT신성장동력핵심기술 사업의 일환으로 수행하였음. [2008-S-042-02, WBAN In-body 시스템 및 On-body 시스템 개발]

* 한국전자통신연구원 융합기술연구부문 WBAN통신연구팀 (ohmik,jyk,hsulee@etri.re.kr)

논문번호 : KICS2009-06-259, 접수일자 : 2009년 6월 25일, 최종논문접수일자 : 2009년 11월 17일

and non-coherent receivers [4],[5], the coherent reception of an IR-UWB packet is required to distinguish a personal area network (PAN) by ternary code, achieve coding gain, and enable better performance for frame timing acquisition [1],[2]. In addition, frequency offset estimation and compensation should be performed in order to obtain the accumulated multipath profile for accurate and reliable ranging^{[1],[2]}.

Although there are several synchronization algorithms for IR-UWB, the algorithms for standard compliant IR-UWB have not yet been proposed. This motivates us to pursue frequency synchronization over multipath channels for IEEE 802.15.4a IR-UWB systems. First, we derive a maximum-likelihood estimation of a frequency offset, for which we incorporate the property of the ternary code. Second, we introduce a closed form of frequency offset estimation aided by the phase difference between preambles, which simplifies hardware implementation.

This paper is organized as follows. In section II, a system model for IR-UWB, as well as a channel model, is presented. The frequency offset estimators are investigated in section III, and a CRLB analysis is carried out in section IV. Simulation results are given in section V, and conclusions are drawn in section VI.

Notation-Upper (lower) bold face letters indicate matrices (column vector). Superscript $(\cdot)^H$ denotes Hermitian conjugate and \otimes kronecker product, and $\lceil \cdot \rceil$ will stand for the upper integer. We will use \mathbf{I}_N to denote the $N \times N$ identity matrix.

II. System Model

Consider an IR-UWB packet of IEEE 802.15.4a described in Fig. 1, which consists of a preamble, start frame delimiter (SFD), PHY header, and payload. Since frequency synchronization should be achieved during preamble reception, we focus on the first part of the IR-UWB frame.

The IEEE 802.15.4a IR-UWB preamble exploits a mandatory ternary code \mathbf{c}_i with a length of 31,

where $i = 1, 2, \dots, 6$. Each code \mathbf{c}_i is a sequence of code symbols drawn from a ternary alphabet $\{-1, 0, 1\}$ and has property of a perfect periodic autocorrelation^[1]. As shown in Fig. 1, the preamble field consists of N_{sync} repetitions of the preamble symbol \mathbf{s}_i , which is given by

$$\mathbf{s}_i = \mathbf{c}_i \otimes \delta_L(n), \quad (1)$$

where $\delta_L(n)$ is the delta function defined as

$$\delta_L(n) = \begin{cases} 1, & n = 0 \\ 0, & n = 1, 2, \dots, L-1 \end{cases} \quad (2)$$

In other words, a preamble symbol \mathbf{s}_i is constructed as depicted in Fig. 1, where $L-1$ zeros are inserted between each ternary element of \mathbf{c}_i . Therefore, the number of chips per preamble symbol can be calculated as $N_c = 31 \cdot L$, and the preamble symbol duration is given by $T_{psym} = N_c \cdot T_c$, where T_c is the chip duration. Figure 1 also illustrates a preamble signal after the UWB pulse shaping on \mathbf{s}_i consisting of 16 pulses, which is repeatedly transmitted through a wireless UWB channel.

Now, let us consider a discrete-time-equivalent baseband model of an IEEE 802.15.4a IR-UWB receiver communicating over a multi-path channel in the presence of a frequency offset. The

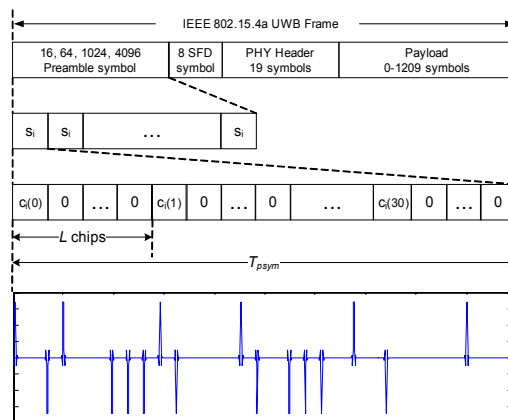


Fig. 1. IEEE 802.15.4a IR-UWB packet

multi-path UWB channel in discrete-time equivalent form is denoted by $h(m)$, $m \in [0, M-1]$, which is a vector containing T_c -spaced samples of the channel response.

Let f_o be the frequency offset (in Hz), which could be due to a mismatch between transmit-receive oscillators. We note here that in IEEE 802.15.4a the oscillator tolerance is ± 20 ppm corresponding to a 180 KHz frequency offset for UWB channel number 3. In the presence of a frequency offset, a received sample at the receiver filter, which is matched to the UWB pulse, can be written as

$$x(n) = e^{j\omega_o n} \sum_{k=0}^{M-1} h(k) s_i(n-k) + w(n), \quad (3)$$

where $\omega_o = 2\pi f_o T_c$ is the normalized frequency offset, and $w(n)$ is zero-mean, white, complex Gaussian distributed noise with variance σ_w^2 .

Assuming a perfect timing acquisition, we can extract the received samples corresponding to the positions where there exist ternary elements of \mathbf{c}_i . This means that sequence (3) is re-sampled by L and serial-to-parallel (S/P) converted into $N \times 1$ blocks with entries $[\mathbf{x}(k)]_n := x(Nk + Ln)$. Selection of the block size $N \times 1$ equivalent to multiples of the ternary code length leads to the following vector-matrix input-output relationship:

$$\mathbf{x}(k) = e^{jN\omega_o k} \mathbf{D}_N(\omega_o) \mathbf{C}_i \bar{\mathbf{h}} + \mathbf{w}(k), \quad (4)$$

where $\mathbf{D}_N(\omega_o)$ is an $N \times N$ diagonal matrix

$$\mathbf{D}_N(\omega_o) = \text{diag}\{1, e^{jL\omega_o}, \dots, e^{j(N-1)L\omega_o}\}. \quad (5)$$

The re-sampled channel in (4) is $\bar{\mathbf{h}} = [h(0), h(L), \dots, h(Q-1)]^T$ for $Q = M/L$. The matrix \mathbf{C}_i is a $N \times Q$ circular matrix with entries

$$[\mathbf{C}_i]_{p,q} = \mathbf{c}_i((p-q)_N), 0 \leq p \leq N-1, 0 \leq q \leq Q-1, \quad (6)$$

where $(p-q)_N$ means “ $p-q$ modulo N .”

We deduce from (4) that estimating the frequency offset is a nonlinear problem since the unknown parameters, frequency offset ω_o and channel $\bar{\mathbf{h}}$, are not simply decoupled. Given the observations \mathbf{x} and the known ternary code \mathbf{c}_i , our goal is to estimate over a multipath channel in IEEE 802.15.4a IR-UWB systems.

III. Frequency Offset Estimation

In this section, we propose techniques of frequency offset estimation. We first derive a simplified ML method. We then investigate a closed form of the frequency offset estimator aided by a phase difference at low-complexity.

3.1 Simplified ML method

Before we derive the estimator, we first examine the property of matrix \mathbf{C}_i . Since the column vector of matrix \mathbf{C}_i , defined as $\bar{\mathbf{c}}_i$, has a property of perfect periodic autocorrelation, it is easy to derive the following^[7]

$$\mathbf{C}_i^H \mathbf{C}_i = \bar{N} \cdot \mathbf{I}_N, \quad (7)$$

where \bar{N} indicates the number of non-zeros in $\bar{\mathbf{c}}_i$.

On the other hand, we consider $k=0$ in (4) and drop the index k for simplicity, resulting in

$$\mathbf{x} = \mathbf{D}_N(\omega_o) \mathbf{C}_i \bar{\mathbf{h}} + \mathbf{w}. \quad (9)$$

For a given $(\omega_o, \bar{\mathbf{h}})$, the observation vector \mathbf{x} is Gaussian with mean $\mathbf{D}_N(\omega_o) \mathbf{C}_i \bar{\mathbf{h}}$ and covariance matrix $\sigma_w^2 \mathbf{I}_N$. Thus, the log-likelihood for the parameter takes the form ^{[6],[7]}:

$$\begin{aligned} \ln p(\mathbf{x} | \omega_o, \bar{\mathbf{h}}) &= N \ln(2\pi\sigma_w^2) \\ &- \frac{1}{\sigma_w^2} [\mathbf{x} - \mathbf{D}_N(\omega_o) \mathbf{C}_i \bar{\mathbf{h}}]^H [\mathbf{x} - \mathbf{D}_N(\omega_o) \mathbf{C}_i \bar{\mathbf{h}}]. \end{aligned} \quad (10)$$

Based on the log-likelihood function, we aim at

maximizing $\ln p(\mathbf{x}|\omega_o, \bar{\mathbf{h}})$ over ω_o and $\bar{\mathbf{h}}$.

If the frequency offset was absent, i. e., $\omega_o = 0$, then we could easily estimate the sampled channel $\bar{\mathbf{h}}$ from the received block (4), which is as follows:

$$\hat{\bar{\mathbf{h}}} = (\mathbf{C}_i^H \mathbf{C}_i)^{-1} \mathbf{C}_i^H \mathbf{x}. \quad (11)$$

In the presence of a frequency offset, we consider ω_o as fixed unknown $\tilde{\omega}_o$, which results in

$$\hat{\bar{\mathbf{h}}} = (\mathbf{C}_i^H \mathbf{C}_i)^{-1} \mathbf{C}_i^H \mathbf{D}_N^H(\tilde{\omega}_o) \mathbf{x}. \quad (12)$$

Substituting (12) into (10), it is derived that maximizing (10) is equal to maximizing the following function

$$g(\tilde{\omega}_o) = \mathbf{x}^H \mathbf{D}_N(\tilde{\omega}_o) \mathbf{B} \mathbf{D}_N^H(\tilde{\omega}_o) \mathbf{x}, \quad (13)$$

where \mathbf{B} is defined as

$$\mathbf{B} = \mathbf{C}_i (\mathbf{C}_i^H \mathbf{C}_i)^{-1} \mathbf{C}_i^H = \frac{1}{N} \mathbf{C}_i \mathbf{C}_i^H. \quad (14)$$

We observe from (14) that the ML problem is simplified due to an advantage of the ternary code as shown in (7), which is

$$\begin{aligned} g(\tilde{\omega}_o) &= \frac{1}{N} \mathbf{x}^H \mathbf{D}_N(\tilde{\omega}_o) \mathbf{C}_i \mathbf{C}_i^H \mathbf{D}_N^H(\tilde{\omega}_o) \mathbf{x} \\ &= \frac{1}{N} \left| \sum_j \bar{c}_i(j) e^{jL(j-1)\tilde{\omega}_o} x(j) \right|^2. \end{aligned} \quad (15)$$

This can be verified by QR factorization of $\mathbf{C}_i \mathbf{C}_i^H$. Consequently, the frequency offset estimate can be found by maximizing $g(\tilde{\omega}_o)$, which is given by

$$\hat{\omega}_o = \arg \max g(\tilde{\omega}_o). \quad (16)$$

We note from (15) and (16) that the frequency offset can be estimated by shifting the phase in

order to maximize the received signal energy correlated by the ternary code.

3.2 Closed-form method

Although the simplified ML frequency offset estimator for an IEEE 802.15.4a system is well derived, it requires a grid search, which makes it difficult to implement (16) in hardware, i.e., in a field-programmable gate array (FPGA) or application-specific integrated circuit (ASIC).

Here, we focus on the implementation of the frequency offset estimator at a comparable performance with an ML estimator. Thanks to repetition of the preamble symbols in (4), we observe that the preamble signals are altered in exactly the same way by a phase shift proportional to the frequency offset. By considering two consecutive preamble symbols, alternative measurements can therefore be obtained as follows:

$$\begin{aligned} \mathbf{x}(k) &= e^{jNk\omega_o} \mathbf{D}_N(\omega_o) \mathbf{C}_i \bar{\mathbf{h}} + \mathbf{w}(k), \\ \mathbf{x}(k+1) &= e^{jN(k+1)\omega_o} \mathbf{D}_N(\omega_o) \mathbf{C}_i \bar{\mathbf{h}} + \mathbf{w}(k+1). \end{aligned} \quad (17)$$

Based on (17), we define the following

$$\begin{aligned} y(k) &= \mathbf{x}^H(k) \mathbf{x}(k+1) \\ &= e^{j\omega_o} \cdot \bar{N} \cdot |h|^2 + \hat{w}(k) + \tilde{w}(k), \end{aligned} \quad (18)$$

where $\hat{w}(k)$ is Gaussian with $N(0, \bar{N} \cdot |h|^2 \cdot \sigma_n^2)$ and $\tilde{w}(k)$ is also Gaussian with $N(0, \bar{N} \cdot \sigma_n^2/2)$.

By considering $\hat{w}(k) + \tilde{w}(k)$ being Gaussian, (18) yields another ML solution for ω_o :

$$\hat{\omega}_o = \tan^{-1} \left\{ \frac{\Im[y(k)]}{\Re[y(k)]} \right\}. \quad (19)$$

Notice that (19) turns out to be a phase difference estimator for the consecutive preamble symbols and gives the closed form estimate of ω_o . This also should be intuitively expected since in the absence of noise, the phase of $\mathbf{x}^H(k) \mathbf{x}(k+1)$ equals ω_o . We also note that the

accuracy of the frequency offset estimator increases as the number of preamble symbols involved in (17), i.e., k , increases. Assuming K preambles in (17), the frequency offset estimator follows in closed form:

$$\hat{\omega}_o = \tan^{-1} \left\{ \frac{\sum_{k=1}^{K-1} \mathcal{I}[y(k)]}{\sum_{k=1}^{K-1} \mathcal{R}[y(k)]} \right\}, \quad (20)$$

which enables realization in hardware at low-complexity.

At this point, someone might raise a question about the effect of the phase noise induced by timing jitter on our estimators. Although the jitter can give timing variation on samples in (17), the effect is negligible since it shows several tens of pico seconds in general. Moreover, the effect of phase noise decreases for large K in (20) due to averaging.

3.3 Summary

We have presented frequency offset estimators for IEEE 802.15.4a IR-UWB signals. In the following, we summarize the algorithms.

Two remarks are now in order.

Remark 1: Although the closed form estimator in (20) has lower complexity than the simplified ML estimator in (16), the simplified ML method achieves high spectral efficiency: the minimum number of preamble symbols for frequency offset estimation is one, while the closed form estimator requires at least two.

Remark 2: The estimators are shown to be independent of the channels. Although we start our derivation of frequency offset estimation with multipath UWB channels, we end up with (16) and (20).

IV. Performance Analysis

To benchmark the performance of our estimators, we derive the Cramer-Rao Lower Bounds (CRLB) of the frequency offset. The

CRLB for the frequency offset estimator is defined as [7]:

$$\text{CRLB}_{\omega_o} = \left(E \left[\left| \frac{\partial \ln p(\mathbf{x}|\omega_o, \mathbf{h})}{\partial \omega_o} \right|^2 \right] \right)^{-1}. \quad (21)$$

By differentiating (10) with respect to ω_o , we obtain

$$\frac{\partial \ln p(\mathbf{x}|\omega_o, \mathbf{h})}{\partial \omega_o} = -\frac{2}{\sigma_w^2} \mathcal{I}(\mathbf{w}^H \bar{\mathbf{D}} \mathbf{D}_N(\omega_o) \mathbf{C} \mathbf{h}), \quad (22)$$

where $\bar{\mathbf{D}} = \text{diag}[0, 1, \dots, N-1]$. Thus the Fisher information of the frequency offset is given as

$$E \left[\left| \frac{\partial \ln p(\mathbf{x}|\omega_o, \mathbf{h})}{\partial \omega_o} \right|^2 \right] = \frac{1}{\sigma_w^2} \text{tr}[\bar{\mathbf{D}} \mathbf{C} \mathbf{R}_h \mathbf{P}^H \bar{\mathbf{D}}], \quad (23)$$

where $\mathbf{R}_h = E[\mathbf{h} \mathbf{h}^H]$. As a result, the CRLB of the frequency offset estimator is given as the inverse of the Fisher information.

$$\text{CRLB}_{\omega_o} = \left(\frac{1}{\sigma_w^2} \text{tr}[\bar{\mathbf{D}} \mathbf{C} \mathbf{R}_h \mathbf{C}^H \bar{\mathbf{D}}] \right)^{-1}. \quad (24)$$

We observe from (24) that as the number of preamble symbols (thus N) increases, the CRLB for the frequency offset decreases.

V. Simulations and Implementation

We conduct simulations to verify the performance of our frequency offset estimator and determine the important parameters for our IEEE 802.15.4a IR-UWB ranging system. We consider both AWGN channel and IEEE 802.15.4a multipath channel models, i. e., CM1 and CM2 [8]. We note that the type of CM1 corresponds to the resident line-of-sight (LOS), and CM2 corresponds to the resident hard none-LOS (NLOS) including concrete walls, which shows the highest attenuation among the multipath channel models.

In all experiments, we use the IEEE 802.15.4a IR-UWB packet as in Fig. 1, and a reference root-raised cosine pulse with an 18 dB bandwidth of approximately 400 MHz^[1]. We also note that we conduct a fixed-point simulation for implementation purpose, i.e., the effect of analog-to-digital converter (ADC) and finite bit-resolution for signal processing are considered in simulation. At the ADC, the received IR-UWB baseband signal is sampled at 998.4 MHz, which is twice the mandatory chip rate $T_c = 1/499.2$ MHz for the IEEE 802.15.4a standard. The other parameters are the following: $N_{sync} = 64$, $L = 16$, $i = 5$, and $N_c = 496$ with the mandatory chip rate. We define $SNR = E_p / \sigma_w^2$, with E_p denoting the energy per pulse. The frequency offsets are uniformly selected in the range [0, 180 KHz] for channel band 3, whose center frequency is 4492.8 MHz^[1]. We note that the frequency offset of 180 KHz is corresponding to 40 ppm in channel band 3.

Example 1 (required ADC bit resolution) - The first consideration is the ADC bit resolution, since it affects the power consumption and performance. In general, a FLASH converter is used for high-speed ADC, where a B -bit Flash converter uses 2^B comparators, so its power and area scale exponentially with the bit resolution. Therefore, the minimum number of bits for the ADC is a critical parameter for the system. To examine the required bit resolution for our estimators, we compared the average normalized mean square error (NMSE) performance of the simplified ML (denoted as “sML”) estimator according to the bit resolutions of ADC in an AWGN channel. The NMSE of ω_o is defined as: $E[\|\hat{\omega}_o - \omega_o\|^2] / \|\omega_o\|^2$. In this simulation, the number of preamble is two, i.e., $N = 62$. Figure 2 shows the NMSE performance of the “sML” estimator corresponding to ADC bit resolutions of 3-bit, 4-bit, 5-bit, and 10-bit. It is observed that 4-bit ADC is enough to achieve the NMSE performance at low-complexity.

Example 2 (performance in AWGN) - Figure 3 compares the “sML” method with the

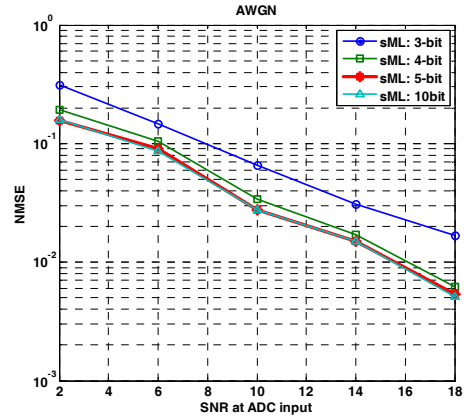


Fig. 2. NMSE performance of simplified ML estimator vs. ADC bit resolutions in AWGN

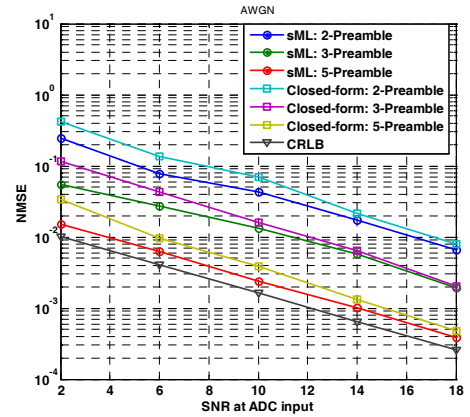


Fig. 3. NMSE performance of the simplified ML & closed-form estimators vs. the number of preambles

“closed-form” method in AWGN. In order to achieve a fair comparison, we use the same number of preambles for both algorithms. Thanks to the result in Fig. 2, we considered 4-bit ADC in this simulation. As shown in Fig. 3, the gap between the “sML” and “closed-form” is relatively small, which means that the “closed-form” method for implementation is suitable for our system. The CRLB in (24) is also drawn as a benchmark.

Example 3 (performance in multipath channels)

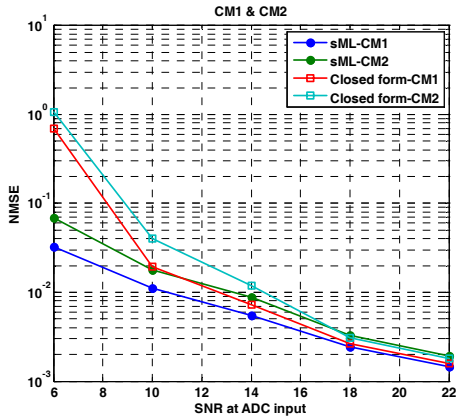


Fig. 4. NMSE performance in CM1 and CM2

-Figure 4 depicts an NMSE of ω_o in IEEE 802.15.4a multipath channels. Although the IEEE 802.15.4a standard supports 9 multipath channel models, we only consider CM1 and CM2. As mentioned earlier, channel model CM2 shows the highest attenuation. In this simulation, we considered 4-bit resolution for the ADC and 5 preambles for the estimator as investigated in Figs. 2 and 3. We notice from Fig. 4 that the performance gap between CM1 and CM2 is relatively small for high SNRs.

Based on Figs. 2, 3 and 4, we infer that the “closed-form” method with 5-preamble and 4-bit ADC is proper for our IEEE 802.15.4a IR-UWB system to mitigate the frequency offset of 180 KHz (40 ppm). In accordance with Figs. 2, 3 and 4, we realized the “closed-form” estimator in FPGA and ASIC at low-complexity, where 16 complex multipliers, 15 adders, and 4 moving average filters are required. We also note that the operation clock for our estimator is relatively low, i.e., approximately 1 MHz, due to its preamble repetition rate $1/T_{psym}$.

VI. Conclusions

We derived frequency offset estimators for IEEE 802.15.4a IR-UWB ranging systems. We have shown that exploiting the property of a ternary code leads to a simplified ML estimator of the frequency offset. For implementation

purpose, we also derived a closed-form estimator whose performance is comparable with the simplified ML estimator in AWGN and multipath channels. Finally, we confirmed the closed-form estimator with 5-preamble and 4-bit ADC for implementation.

References

- [1] IEEE 802.15 TG4a, “Part 15.4: Wireless medium access control and physical layer specifications for low-rate wireless personal area networks (WPANs),” *IEEE Std 802.15.4a™*, Aug. 2007.
- [2] Z. Sahinoglu and S. Gezici, “Ranging in the 802.15.4a standard,” *IEEE WAMICON 2006*, pp.1-5, Dec. 2006.
- [3] W. Zhang, H. Shen, Z. Bai, et al., “Impulse series for UWB-based cognitive radio system,” *ETRI Journal*, Vol.29, No.4, pp.521-523, Aug. 2007.
- [4] N. He, and C. Tepedelenioglu, “Performance analysis of non-coherent UWB receivers at different synchronization levels,” *IEEE Trans. on wireless comm.*, Vol.5, No.6, pp.1266-1273, June 2006.
- [5] J. Ryckaert, G. Van der Plas, V. De Heyn, et al., “A 0.65-to-1.4nJ/burst 3-to-10GHz UWB digital TX in 90nm CMOS for IEEE 802.15.4a,” *IEEE ISSCC 2007*, pp.120-591, Feb. 2007.
- [6] M. Morelli and U. Mengali, “Carrier-frequency estimation for transmissions over selective channels,” *IEEE Trans. on Comm.*, Vol.48, No.9, pp.1580-1589, Sept. 2000.
- [7] T. K. Moon and W. C. Stirling, *Mathematical methods and algorithms for signal processing*, Prentice Hall, 2000.
- [8] A. F. Molisch, K. Balakrishnan, D. Cassioli, C. -C. Chong, S. Emami, A. Fort, J. Karedal, J. Kunisch, H. Schantz, U. Schuster and K. Siwiak, “IEEE 802.15.4a channel model - final report,” *IEEE P802.15-04/662r2-TG4a*, July 2005.

오 미 경 (Mi-Kyung Oh)

정회원



2000년 2월 중앙대학교 전기
전자제어공학부
2002년 2월 한국과학기술원 전
자전산학과 석사
2006년 2월 한국과학기술원 전
자전산학과 박사
2006년 3월~현재 한국전자통
신연구원 선임연구원

<관심분야> WPAN, WBAN, IR-UWB, 무선측위
시스템, 통신신호처리

이 형 수 (HyungSoo Lee)

정회원



1980년 2월 경북대학교 전자
공학과
1986년 2월 연세대학교 전자계
산학 석사
1996년 2월 성균관대학교 정보
공학 박사
1983년 4월~현재 한국전자통신
연구원 책임연구원

<관심분야> WBAN, WPAN, 전파전파특성, 주파수
할당 및 간섭 평가

김 재 영 (Jae-young Kim)

정회원



1990년 2월연세대학교 전자 공
학과
1992년 2월 연세대학교 전자
공학과 석사
1996년 8월 연세대학교 전자
공학과 박사
1999년~현재 한국전자통신연구
원 책임연구원

<관심분야> WPAN, WBAN, IR-UWB, ZigBee, 무
선측위 시스템, Analog/RFIC 설계